# Performance Analysis of a Designed 635*nm* Compressively Strained Red Laser under Variant Temperature Condition

Tawsif Ibne Alam
Department of EEE, Faculty of Engineering,
American International University-Bangladesh (AIUB)
Banani, Dhaka-1213, Bangladesh
tawsif.ibne.alam@gmail.com

Rinku Basak
Department of EEE, Faculty of Engineering,
American International University-Bangladesh (AIUB)
Banani, Dhaka-1213, Bangladesh
rinku_biju@yahoo.com

***Abstract*—In this work, the effects of temperature on the output power and modulation response of a designed 635*nm* Red Laser have been theoretically determined. At 300*K*, for a $Ga_{0.48}In_{0.52}P/(Al_{0.36}Ga_{0.64})_{0.52}In_{0.48}P$ compressively strained MQW Red Diode Laser, the maximum steady state output power has been found out as 105.9*mW* at an injection current of 90*mA*, with a threshold current as low as 8.8*mA*. Furthermore, increase in temperature reveals a red shift of power vs. wavelength characteristics and intensity fluctuation with a peak intensity at 639.8*nm* at 330*K* temperature, decrease in overall output power, increase in threshold current and a maximum -3dB modulation bandwidth of 18.3 GHz at a temperature of 300*K*.**

***Keywords—Red Laser; Temperature; Output Power; Modulation bandwidth;***

## I. INTRODUCTION

Red Laser Diodes in the range of 630*nm*-670*nm* has been widely used in consumer and professional applications that include optical disk recording [1-2], sensor applications [3], photodynamic therapy [2-7], laser display and pointer technology [7-8] and solid state laser pumping [7].

Demonstration of GaInP/AlGaInP Red laser diode system was first made during 1985 [9-10]. However, because of thermal leakage at elevated temperature and power, their performance characteristics has been found to degrade, with liner increase of threshold current and decrease of external differential quantum efficiency with increasing temperature above threshold. These unwanted characteristics become particularly pronounced as the operating wavelength is reduced and they present one of the major barriers to the reproducible fabrication of devices in the region of 630*nm*.

Semiconductor heterostructures employ quantum confinement, alloy composition, and mismatch strain to achieve diverse electronic and optical properties. This versatility has been central to the remarkable progress in device science made during the past three and half decades. A prime example is the double heterojunction diode laser, in which highly efficient laser emission is generated by electron-hole recombination between discrete quantum well (QW) states in an active layer. The need to engineer for optimal efficiency, robustness, lasing frequency, and increased output power has led to a steady growth in heterostructure complexity. Consequently, in order to design and/or model modern optoelectronic devices one requires detailed knowledge of many material parameters. In particular, the heterojunction band discontinuities play a key role. These discontinuities (or band offsets), which determine the confinement of the electrons and holes in the active-layer QWs, depend on the chemical composition of the heterostructure constituents and on the amount and distribution of lattice-mismatch strain.

The concept of a strained layer has been met already in connection with double heterostructure devices. Strain occurs in heterostructures when the lattice parameter of the substrate does not match the lattice parameter of the deposited layer, which therefore deforms in order for the two lattices to register with each other. However, strained layers must be thinner than the critical thickness, after which plastic deformation occurs via the creation of dislocations. These can act as non-radiative recombination centers and in most materials will degrade the laser performance. As the critical thickness may be no more than a few nanometers, strain has to be avoided at all costs in the DH laser, but quantum wells can be fabricated quite easily below the critical thickness. Such layers are therefore stable and can be used to construct diode lasers, even for operation at high power with good operational stability.

Strained layer lasers exhibit improved performance over lattice matched lasers, principally because of the effect of strain on the valence band. Strain in bulk material alters the band gap and lifts the degeneracy of the light and heavy hole bands. The effect of quantum confinement, which is to separate these states according to effective mass, is superimposed on this initial separation. The peak in the gain spectrum is shifted in wavelength to match the band gap, so the well width has to be different from that in unstrained material of the same composition to give a specified output wavelength.

In compressively strained materials the band gap is increased and the light hole band is pushed deeper relative to the heavy hole [11]. Therefore the quantum confined heavy hole and light hole states are even further apart in energy. Furthermore, the heavy hole states have their in-plane effective mass reduced, thereby reducing the density of states. The band mixing effects in compressively strained lasers are much reduced by the greater separation and the valence band

therefore approximates much more to a parabolic dependence of energy on wavevector than in the unstrained case. This further reduces the density of states, especially in narrow wells.

In this work, the performance characteristics of a designed 635*nm* compressively strained Multi Quantum Well (MQW) Red laser diode has been analyzed and presented with the motivation of the fact that compressively strained quantum well lasers provide lower operating threshold conditions. The designed laser has been further subjected to a variant temperature condition and the expected output results have been presented.

## II. Device Structure and Design

The active region of a 635*nm* Red Laser diode, as presented in *Fig.1*, consists of 3 Quantum Wells(QW) of $Ga_{0.48}In_{0.52}P$ of 7.3*nm* each having compressively strained to two barriers of $(Al_{0.36}Ga_{0.64})_{0.52}In_{0.48}P$ of 9*nm* each. The active region is sandwiched by two separate confinement heterostructure (SCH) layers of $(Al_{0.36}Ga_{0.64})_{0.52}In_{0.48}P$ of 80*nm*. The concentration of layers are chosen in such a way to achieve a peak wavelength around 635*nm*.

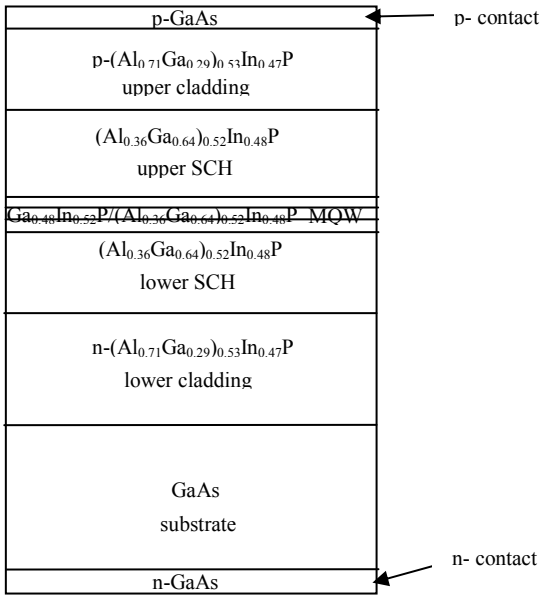


Fig. 1. The structure of a designed 635*nm* MQW Red Laser.

The volume of the active region is $5.985 \times 10^{-11} cm^3$. The total thickness ($d$) of the active region is 39.9*nm* in the x-y plane considering 3 QWs and 2 barriers. The length($L$) and width($w$) of the device is 750$\mu m$ in x-z-plane and 2$\mu m$ in y-z-plane respectively.

The total thickness of the cavity including the wave guiding region is calculated as 199.9*nm*. The cavity length is same as the active region length and for the same width the cavity volume $V_p$ is calculated as $2.9985 \times 10^{-10} cm^3$. The confinement factor is calculated as $\Gamma = \Gamma_{xy} \times \Gamma_z = 0.1996 \times 1 = 0.1996$. The p-type and n-type cladding layers of $(Al_{0.71}Ga_{0.29})_{0.53}In_{0.47}P$ of 2.2μm each have been used, having lattice matched to the substrate. A n-GaAs substrate of 2μm is connected with the lower n-contact and the upper p-contact is connected with the p-cladding layer as shown in *Fig. 1*. The material constants are presented in Table-1 from [7-8], [10-16].

## III. Simulation And Results

The transparency carrier density ($N_{tr}$) of a material is related to the effective masses of carriers in the conduction band (CB) and valance band (VB) as [11]:

$$N_{tr} = 2\left(\frac{kT}{2\pi\hbar^2}\right)^{3/2}(m_c m_v)^{3/4} \qquad (1)$$

where, $k$ is the Boltzmann constant, $T$ is the temperature in Kelvin, $\hbar$ is the rationalized Planck's constant, $m_c$ and $m_v$ are the effective masses of the carriers in the CB and VB respectively.

The transparency carrier density ($N_{tr}$) is calculated as $2.1378 \times 10^{18} cm^{-3}$. A high peak material gain with lower transparency carrier density of a QW material is required for designing a semiconductor laser and for this reason, $Ga_{0.48}In_{0.52}P$ has been chosen as the active region material.

### A. Computation of Material Gain

The material gain, $g$, of a 635*nm* compressively strained Red Laser can be found out using [11]:

$$g(E) = \left(\frac{q^2\pi\hbar}{\varepsilon_0 m_0{}^2 n_r c E}\right)|M_T|^2 \rho_r (f_2 - f_1) \quad (2)$$

where, $q$ is the electronic charge, $\varepsilon_0$ is the free space permittivity, $c$ is the speed of light, $n_r$ is the refractive index of the laser structure, $E$ is the transition energy, $m_0$ is the stationary mass of electron, $|M_T|^2$ is the square of the transition momentum matrix element, $\rho_r$ is the reduced density of state, $\hbar$ is the Planck's constant divided by 2π, $f_2$ and $f_1$ are quasi-Fermi functions in the conduction and valance band respectively.

Using equation (2), at 300$K$ the material gain for a 635*nm* $Ga_{0.48}In_{0.52}P/(Al_{0.36}Ga_{0.64})_{0.52}In_{0.48}P$ compressively strained MQW Red Laser is obtained and presented in *Fig.2*. The peak material gain of the device has been obtained as $1908 cm^{-1}$ around the lasing wavelength of 634*nm.*

TABLE I. Material Parameters of **GaP**, **InP** and **AlP** Used in Calulation of **GaInP** and **AlGaInP** Constants

| Material System and Compositions | Parameters | | | | | | | | | |
|---|---|---|---|---|---|---|---|---|---|---|
| | $E_g$ | $a_c$ | $m_c/m_0$ | $m_{hh}/m_0$ | $n$ | $C_{11}$ | $C_{12}$ | $a_c$ | $a_v$ | $b$ |
| GaP | 2.7770 | 5.4505 | 0.13 | 0.3257 | ---- | 14.05 | 6.20 | -8.2 | -1.7 | -1.6 |
| InP | 1.3529 | 5.8697 | 0.0795 | 0.532 | ---- | 10.11 | 5.61 | -6.0 | -0.6 | -2.0 |
| AlP | 3.5527 | 5.4672 | 0.22 | 0.518 | ---- | ---- | ---- | ---- | ---- | ---- |
| $Ga_{0.48}In_{0.52}P$ | 1.8742 | 5.6685 | ---- | ---- | 3.6 | ---- | ---- | ---- | ---- | ---- |
| $(Al_{0.36}Ga_{0.64})_{0.52}In_{0.48}P$ | 2.2037 | 5.6633 | ---- | ---- | 3.23 | ---- | ---- | ---- | ---- | ---- |

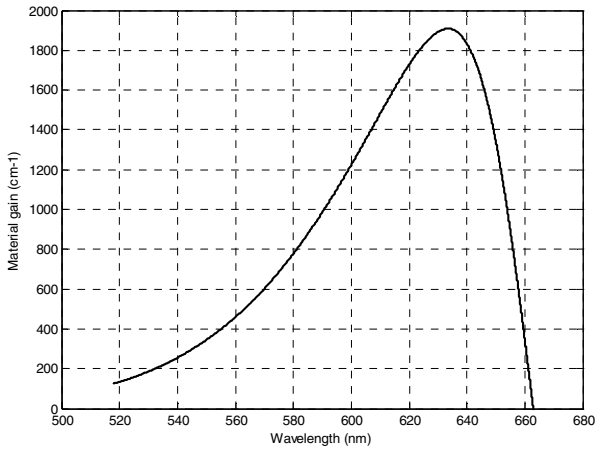


Fig. 2. Plot of material gain vs. wavelength of the designed $Ga_{0.48}In_{0.52}P/(Al_{0.36}Ga_{0.64})_{0.52}In_{0.48}P$ 3QW Red laser at 300*K*. The material gain of the designed laser varies with the variation of wavelength and a peak material gain is obtained as $1908cm^{-1}$ at $634nm$ wavelength.

Considering the calculation of material gain, solution of rate equations, calculations of output power, power vs. wavelength characteristics and analysis of modulation response using MATLAB simulator are presented.

Taking into account the effect of strain and quantum confinement in the $Ga_{0.48}In_{0.52}P$ quantum wells, the conduction subband's energy shifted with the hydrostatic strain is given by [15-16]:

$$E_n(k_{||}) = E_n + \frac{\hbar^2}{2m_c}{k_{||}}^2 + 2a_c\left(\frac{C_{11}-C_{12}}{C_{11}}\right)\varepsilon_{||} \qquad (3)$$

where $a_c$ is the hydrostatic deformation potential of the conduction band, $C_{11}$ and $C_{12}$ are elastic stiffness constants, $\varepsilon_{||}$ is the biaxial strain in the well plane, $E_n$ is the eigenvalue of the finite quantum well, $m_c$ is the electron effective mass, $k_{||}$ is the wave vector in the well plane.

The valance subband's energy dispersions are obtained by using the unitary transformed Luttinger-Kohn Hamiltonian with strain as follows [15-16]:

$$H = \begin{bmatrix} P+Q+H^{\varepsilon}{}_{HH} & \tilde{R} & 0 & 0 \\ \tilde{R}^* & P-Q+H^{\varepsilon}{}_{LH} & 0 & 0 \\ 0 & 0 & P-Q+H^{\varepsilon}{}_{LH} & \tilde{R} \\ 0 & 0 & \tilde{R}^* & P+Q+H^{\varepsilon}{}_{HH} \end{bmatrix} + V(z) \qquad (4)$$

where

$$P = \frac{1}{2}\left(\frac{\hbar^2}{m}\right)\gamma_1\left({k_{||}}^2 - \frac{\partial^2}{\partial z^2}\right)$$

$$Q = \frac{1}{2}\left(\frac{\hbar^2}{m}\right)\gamma_2\left({k_{||}}^2 + 2\frac{\partial^2}{\partial z^2}\right)$$

$$\tilde{R} = \left(\frac{\hbar^2}{m}\right)\left(\frac{\sqrt{3}}{2}\bar{\gamma}{k_{||}}^2 - i\left\{\sqrt{3}\gamma_3 k_{||}\frac{\partial}{\partial z}\right\}\right)$$

$$H^{\varepsilon}{}_{HH} = 2a_v\left(\frac{C_{11}-C_{12}}{C_{11}}\right)\varepsilon_{||} - b\left(\frac{C_{11}+2C_{12}}{C_{11}}\right)\varepsilon_{||}$$

$$H^{\varepsilon}{}_{LH} = 2a_v\left(\frac{C_{11}-C_{12}}{C_{11}}\right)\varepsilon_{||} + b\left(\frac{C_{11}+2C_{12}}{C_{11}}\right)\varepsilon_{||}$$

$$\bar{\gamma} = \frac{1}{2}(\gamma_2 + \gamma_3)$$

where $\gamma_1$, $\gamma_2$ and $\gamma_3$ are Luttinger parameters, $a_v$ is the hydrostatic deformation potential of the valence band, $b$ is the shear deformation potential, and $m$ is the free electron mass. In this model, a finite potential model has been used.

As mentioned earlier, the quantum wells have been compressively strained for which the bands split up, allowing only transition from the conduction band subband to the heavy hole valence subband. So the conduction subband offset can be written as [15]:

$$\Delta E_c = 2a_c\left(\frac{C_{11}-C_{12}}{C_{11}}\right)\varepsilon_{||} + E_n \qquad (5)$$

and the valence band off-set parameter for the heavy hole can be obtained as [15]:

$$\Delta E_{hh} = 2a_v\left(\frac{C_{11}-C_{12}}{C_{11}}\right)\varepsilon_{||} - b\left(\frac{C_{11}+2C_{12}}{C_{11}}\right)\varepsilon_{||} + E_{hn} \qquad (6)$$

where $E_{hn}$ is the heavy-hole eigenvalue of a finite quantum well. The value of $\Delta E_c$ has been obtained as 0.0575eV and that of $\Delta E_{hh}$ as 0.0238eV. The overall transition energy $E_{tr}$ can now be written as:

$$E_{tr}=E_g+\Delta E_c+\Delta E_{hh} \qquad (7)$$

where $E_g$ is the bandgap energy of the bulk $Ga_{0.48}In_{0.52}P$ material.

### *B. Rate Equation Solution and Output Power*

The rate equation of a semiconductor Red Laser has been solved using finite difference method. For solution of rate equation, a threshold carrier density of $2.2506x10^{18}cm^{-3}$ has been found out using the well known expression [11]:

$$N_{th} = N_{tr} \times e^{\frac{(\alpha_i+\alpha_m)}{\Gamma\times g_0}} \qquad (8)$$

The photon lifetime ($\tau_p$) is then obtained as $5.8133ps$ using the following expression [11]:

$$\tau_p = \frac{1}{\left(v_g \times (\alpha_i + \alpha_m)\right)} \qquad (9)$$

from a group velocity $v_g$ of $8.7848x10^{-9}cms^{-1}$. Using the above parameters, the threshold current ($I_{th}$) of the laser has been obtained as 8.8mA, using the well known expression [11]:

$$I_{th} = \frac{q \times V \times N_{th}}{\eta_i \times \tau_c} \qquad (10)$$

The rate equations of a semiconductor laser are presented as [11], [17-18]:

$$\frac{dN}{dt} = \frac{\eta_i I}{qV} - \frac{N}{\tau_c} - \frac{v_g a(N-N_{tr})S}{(1+\varepsilon S)} \qquad (11)$$

$$\frac{dS}{dt} = \frac{\Gamma v_g a(N-N_{tr})S}{(1+\varepsilon S)} + \Gamma\beta_{sp}R_{sp} - \frac{S}{\tau_p} \qquad (12)$$

where, $N$ is the carrier density, $S$ is the photon density, $I$ is the injection current, $V$ is the volume of the active region, $\eta_i$ is the injection efficiency, $\tau_c$ is the carrier lifetime, $v_g$ is the group velocity, $a$ is the differential gain, $\varepsilon$ is the gain saturation

parameter, $\beta_{sp}$ is the spontaneous emission coefficient, $R_{sp}$ is the spontaneous emission rate and $\tau_p$ is the photon lifetime.

Using MATLAB simulator, the solution to the rate equations have been obtained using finite difference method, for a time frame of 0-2.5*ns* approximately, for a chosen (applicable) value of injection current of 90*mA,* the rate of change of carrier density, rate of change of photon density and output power of the designed laser have been found out. At 300*K*, a steady state carrier density of $2.356\text{x}10^{18} cm^{-3}$as shown in *Fig. 3*, a steady state photon density of $8.806\text{x}10^{15} cm^{-3}$ as shown in *Fig. 4* and a steady state output power of 105.9*mW* as shown in *Fig. 5*.

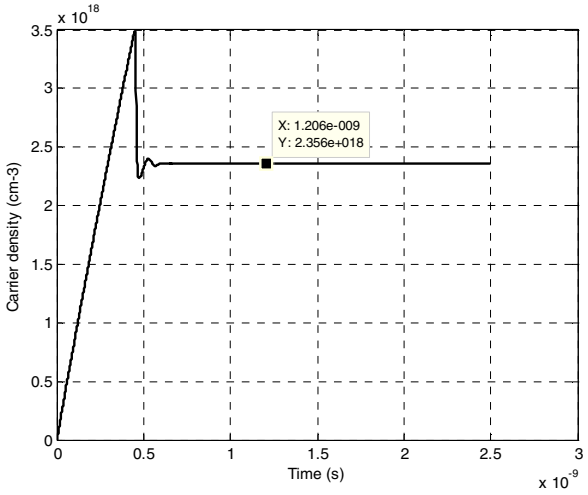


Fig. 3. Plot of carrier density vs. time, for a compressively strained $Ga_{0.48}In_{0.52}P/(Al_{0.36}Ga_{0.64})_{0.52}In_{0.48}P$ 3QW Red laser at 300*K* . The steady state carrier density of the device has been found as $2.356\text{x}10^{18}\text{cm}^{-3}$.

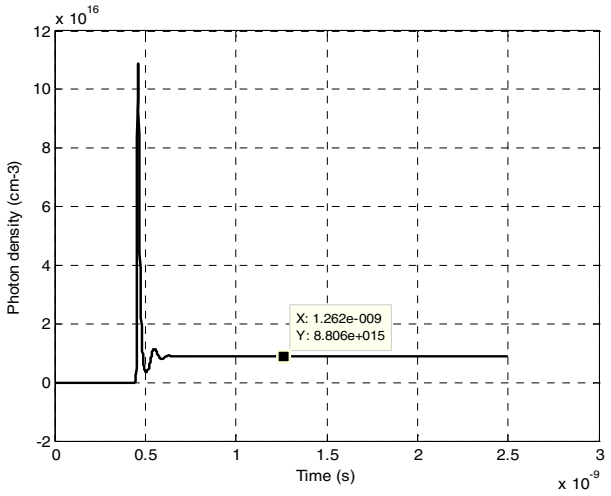


Fig. 4. Plot of photon density vs. time, for a compressively strained $Ga_{0.48}In_{0.52}P/(Al_{0.36}Ga_{0.64})_{0.52}In_{0.48}P$ 3QW Red laser at 300*K* . The steady state photon density of the device has been found as $8.806\text{x}10^{15}\text{cm}^{-3}$.

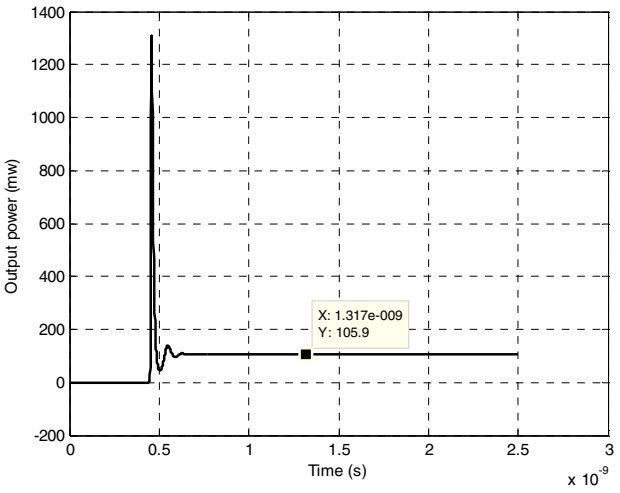


Fig. 5. Plot of output power vs. time, for a compressively strained $Ga_{0.48}In_{0.52}P/(Al_{0.36}Ga_{0.64})_{0.52}In_{0.48}P$ 3QW Red laser at 300*K* . The steady state output power of the device has been found as 105.9mW.

### *C. Effect of Temperature on Performance Characteristics*

The temperature variant bandgap energy can be expressed using the Varshini equation [12], [14]:

$$E_g(T) = E_g(T=0) - \frac{\alpha T^2}{T+\beta} \qquad (13)$$

where α and β are Varshini parameters.

The Output Power of the compressively strained Red Laser can be found out using the varying nature of photon density obtained from the photon rate equation [11]:

$$P_{out} = v_g \alpha_m S h v V_p \qquad (14)$$

With the aid of the varying nature of the photon density simulation, variation of output power has been obtained at temperatures 300*K*, 330*K* and 360*K*.

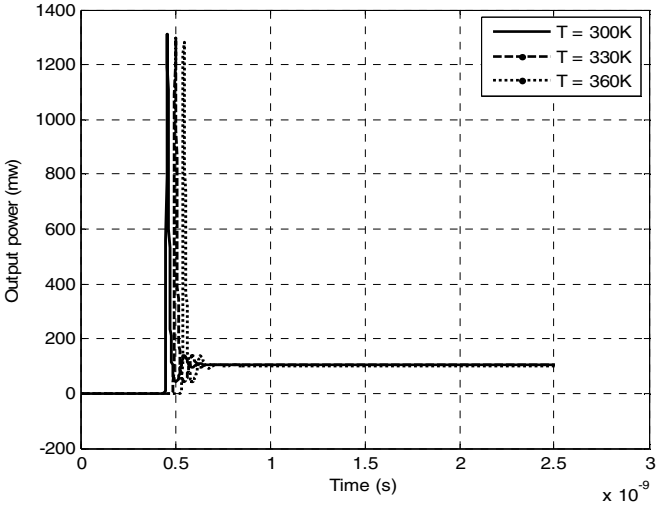


Fig. 6. Plots of output power vs. time of the designed $Ga_{0.48}In_{0.52}P/(Al_{0.36}Ga_{0.64})_{0.52}In_{0.48}P$ 635*nm* Red laser for different temperature values of 300*K*, 330*K* and 360*K*. A maximum steady state output power of 105.9mW has been obtained at 300*K* temperature.

From *Fig. 6* it is seen that the output power of the laser decreases and the turn on delay time increases with increase in temperature and maximum output power has been obtained as 105.9$mW$.

The output power of the designed laser can also be calculated by varying the injection current as [11]:

$$P_o = \frac{\alpha_m h\nu}{qg\Gamma}(I - I_{th}) \qquad (15)$$

where, $g$ is the material gain, $\alpha_m$ is the mirror loss coefficient, $h$ is the Planck's constant, $\nu$ is the lasing frequency, $\Gamma$ is the confinement factor, $I$ is the injection current and $I_{th}$ is the threshold current.

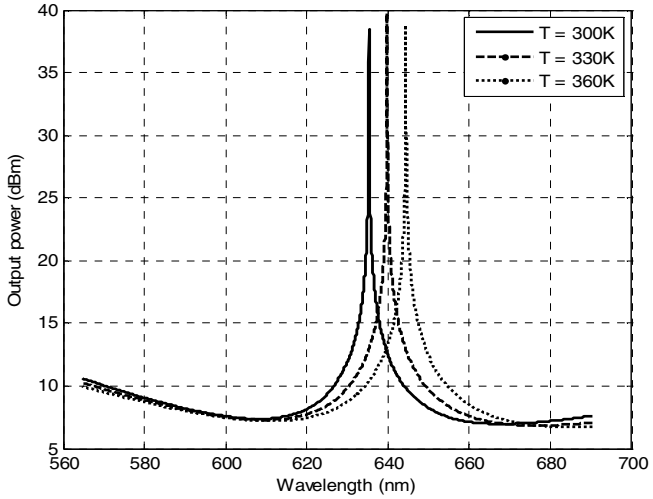


Fig. 7. Plots of output power vs. wavelength characteristics of the designed $Ga_{0.48}In_{0.52}P/(Al_{0.36}Ga_{0.64})_{0.52}In_{0.48}P$ compressively strained 635$nm$ Red laser for different temperature values of 300$K$, 330$K$ and 360$K$. At 300$K$, a peak intensity of 39.73dBm output power has been obtained at 639.8$nm$ .

Using equation (15), for an injection current of 90$mA$, the output power of the red laser is calculated by varying wavelength and the results are presented as shown in *Fig. 7* for a temperature of 300$K$, 330$K$ and 360$K$. The material gain varies with the variation of wavelength which further varies the optical output power of the laser and the peak output power is obtained at 639.8$nm$ wavelength at a temperature of 330K. The obtained result is very close to the calculated value. It is also observed that with increase in temperature, there is a red shift of characteristics wavelength.

Using equation (15), the output power vs. injection current characteristics of the device can also be obtained by varying the injection current from 0 to 90$mA$, for a temperature of 300K, 330K and 360K. This has been plotted and presented in *Fig. 8*.

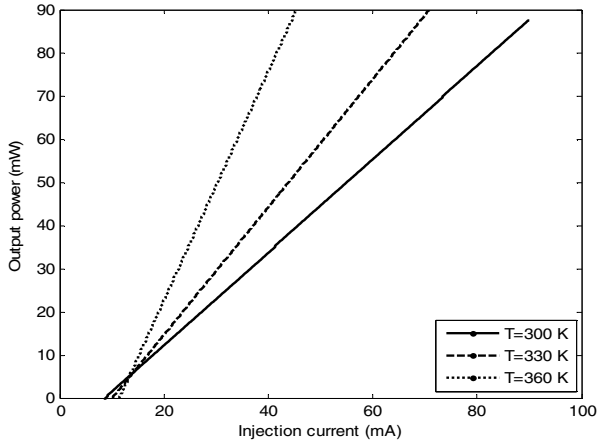


Fig. 8. Plots of output power vs. wavelength characteristics of the designed $Ga_{0.48}In_{0.52}P/(Al_{0.36}Ga_{0.64})_{0.52}In_{0.48}P$ compressively strained 635$nm$ Red laser for different temperature values of 300$K$, 330$K$ and 360$K$. At 300$K$, the lowest threshold current of 8.8$mA$ has been observed.

From the above plot, it is seen that with increase in temperature from 300$K$ to 360$K$, the threshold current of the device increases from 8.8 $mA$ to 11.46 $mA$, with also an increment in the gradient of the power vs. injection current characteristics due to the shift of operating wavelength of the device and overall decrease in modal gain.

The modulation response of the designed laser has been obtained using the equation of the transfer function as given below [11]:

$$H(f) = \frac{{f_R}^2}{{f_R}^2 - f^2 + j\frac{f}{2\pi}\gamma} \qquad (16)$$

where, $f_R$ is the resonance frequency and $\gamma$ is the damping parameter of the laser.

The above equation has been used to obtain the plot of relative response vs. frequency for a value of injection current of 90$mA$ as shown in fig. 9 at 300$K$, 330$K$ and 360$K$ temperature.

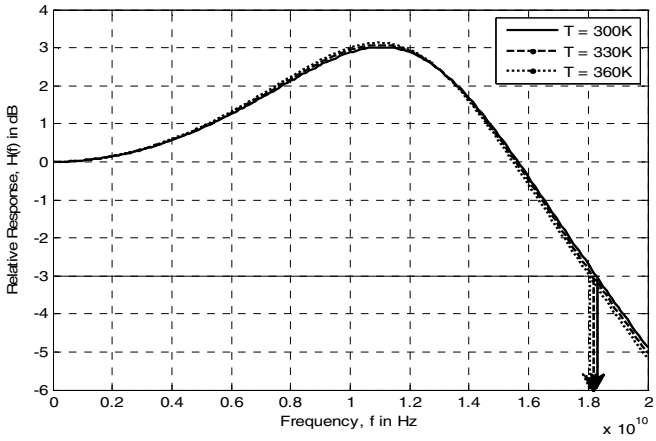


Fig. 9. Plots of output power vs. wavelength characteristics of the designed $Ga_{0.48}In_{0.52}P/(Al_{0.36}Ga_{0.64})_{0.52}In_{0.48}P$ 635$nm$ Red laser for different temperature values of 300$K$, 330$K$ and 360$K$. At 300$K$, the maximum modulation bandwidth of 18.3GHz has been observed.

From *Fig. 9*, it is seen that with increase in temperature from 300K to 360K, both the relaxation resonance frequency and -3dB modulation bandwidth decreases, with a maximum modulation bandwidth of 18.3GHz observed at 300*K* temperature.

## IV. CONCLUSION

In this work, the thickness of the quantum well (QW), separate confinement heterostructure (SCH), and cladding layer along with the length and width of the device have been proposed for a compressively strained MQW 635*nm* Laser. The material gain has been found out for the finalized dimension, and the peak material gain has been used for finding the threshold conditions and solution of rate equations for finding a steady state output power of 105.9*mW*. Furthermore, a temperature dependent analysis of output power vs. time, output power vs. wavelength characteristics, output power vs. current characteristics and modulation response reveals a decrease in output power, red shift of the operating wavelength, increase in threshold current and a decrease in modulation bandwidth with increase in temperature, with a peak wavelength intensity at 639.8*nm* at 330K temperature, a maximum modulation bandwidth of 18.3 GHz and maximum output power of 105.9mW with a threshold current as low as 8.8*mA* at 300*K* temperature. As a result the finalized design has been optimized for a 3 QW structure, and has been proposed to be operated around 300*K* temperature, owing to the fact that temperature dependent non radiative processes like auger recombination and other injection current dependent effects are out of the scope of this research. The device is expected to perform well after fabrication.

## REFERENCES


[1] Bo Lu, E. Vail, J.S. Osinski and B. Schmitt, "High-speed low-parasitic low-divergence 635nm single mode lasers", Electronics Letters, Vol.34, No.18, pp. 1750-1751, 1998.

[2] Peter M. Smowton, Gareth M. Lewis, Peter Blood, and Weng W. Chow, "Optimization of 635-nm Tensile Strained GaInP Laser Diodes", IEEE Journal Of Selected Topics In Quantum Electronics, Vol. 9, No. 5, pp. 1246-1251, 2003.

[3] H.P. Gauggel, R. Winterhoff, J. Kuhn, F. Scholz and H. Schweizer, "Room temperature operation of single mode DBR lasers at 635nm", Electronics Letters, Vol. 33, No.17, pp.1466-1467, 1997.

[4] Ivan Charamisinau, Gemunu S. Happawana, Gary A. Evans, Jay B. Kirk, David P. Bour, Arye Rosen and R. Alexander His, "High-Power Semiconductor Red Laser Arrays for Use in Photodynamic Therapy", IEEE Journal Of Selected Topics In Quantum Electronics, Vol. 11, No.4, pp.881-891, 2005.

[5] Mustafa, F.H., Jaafar, M.S., Ismail, A.H., Houssein, H.A.A. "The effect of laser wavelength in photodynamic therapy and phototherapy for superficial skin diseases", IEEE International Conference on_ Imaging Systems and Techniques (IST), DOI: 10.1109/IST.2011.5962166, pp.232-236, 2011.

[6] Riccardo Rossi, Torello Lotti and Nicola Bruscino, "Photodynamic Therapy/Assisted Photorejuvenation", Journal of Cosmetics, Dermatological Sciences and Applications, Vol-1, No.1, pp.30-35, 2011.

[7] J. M.G. Tijero,H. Odriozola, I. Esquivias, A. Martín-Mínguez, P. Brick, M. Reufer, M. Bou Sanayeh, A. Gomez Iglesias and N. Linder, "Self-Consistent Modeling of Edge-Emitting GaInP/AlGaInP Red Lasers", NUSOD, 978-1-4244-2307-1, pp.73-74, 2008.

[8] C. Y. Liu, Shu Yuan, J. R. Dong, S. J. Chua, M. C. Y. Chan and S. Z. Wang, "Temperature-dependent photoluminescence of GaInP/AlGaInP multiple quantum well laser structure grown by metalorganic chemical vapor deposition with tertiarybutylarsine and tertiarybutylphosphine", Journal Of Applied Physics, Vol. 94, No.5, pp.2962-2967, September 2003.

[9] Bocang Qiu, Stewart McDougall, Dan Yanson "Analysis of thermal performance of InGaP/InGaAlP quantum wells for high-power red laser diodes", NUSOD, 978-1-4244-2307-1, pp.69-70, 2008.

[10] Hajime Okuda, Masayuki Ishikawa, Hideo Shiozawa, Yukio Watanabe, Kazuhiko Itaya, Kouichi Nitta, Gen-Ichi Hatakoshi, Yoshihiro Kokubun and Yutaka Uematsu, "Highly Reliable InGaP/InGaAlP Visible Light Emitting Inner Stripe Lasers with 667nm Lasing Wavelength", IEEE Journal of Quantum Electronics, Vol. 25, No. 6, pp.1477-1482, June 1989.

[11] L. A. Coldren and S.W. Corzine, Diode Lasers and Photonic Integrated Circuits, John Wiley & Sons, Inc, pp. 1-263, 527-535, 1995.

[12] I. Vurgaftman and J. R. Meyer, L. R. Ram-Mohan, "Band parameters for III–V compound semiconductors and their alloys", Journal of Applied Physics, Vol. 89, No. 11, pp. 5851-5862, 2001.

[13] Weng W. Chow, Stephan W. Koch, Semiconductor-Laser Fundamentals Physics of the Gain Materials, ISBN 3-540-64166-1 Springer-Verlag Berlin Heidelberg New York, pp. 1-225, 1999.

[14] Sadao Adachi, Properties of group-IV, III–V and II–VI Semiconductors, John Wiley & Sons, ISBN 0-470-09032-4, pp. 11-359, 2005.

[15] Yongqin Yu, Xiaoyang Zhang, Baibiao Huang, Duxiang Wang, Jiyong Wei, Hailong Zhou, Jiaoqing Pan, Yun Qi, Wenlan Chen, Xiaoyan Qin, Zhongxiang Ren,"Strain effect and characteristics of GaInP/AlGaInP strain compensated multiple quantum wells", Materials Science and Engineering, B97, pp.211-216, 2003.

[16] Satoshi Kamiyama, Takeshi Uenoyama, Masaya Mannoh, Yuzaburoh Ban and Kiyoshi Ohnaka, "Analysis of GaInP/AlGaInP Compressive Strained Multiple-Quantum-Well Laser", IEEE Journal Of Quantum Electronics. Vol. 30. No. 6 , pp.1363-1369, 1994.

[17] Toby Schaer, Robert Rusnov, Stephen Eagle, Jay Jastrebski, Steven Albanese and Xavier Fernando "A Dynamic Simulation Model for Semiconductor Laser Diodes", CCECE, pp. 293-297, 2003.

[18] Xing Dezhi, Wang Wenzhe, Jin Xiaoli, Su Jing and Liu Hongxia, "A Numerical Model for Semiconductor Laser Diodes", Symposium on Photonics and Optoelectronics (SOPO), DOI:10.1109/SOPO.2012.6271033, pp. 1-4, 2012.